Published in final edited form as:
Biol Psychiatry. 2011 July 1; 70(1): 43–50. doi:10.1016/j.biopsych.2011.02.010.

Variable Global Dysconnectivity and Individual Differences in Schizophrenia

Michael W. Cole, **Alan Anticevic**, **Grega Repovs**, and **Deanna Barch**
Department of Psychology (MWC, AA, DB), Washington University, St. Louis, Missouri; and the Department of Psychology (GR), University of Ljubljana, Ljubljana, Slovenia.

Abstract

Background—A fundamental challenge for understanding neuropsychiatric disease is identifying sources of individual differences in psychopathology, especially when there is substantial heterogeneity of symptom expression, such as is found in schizophrenia (SCZ). We hypothesized that such heterogeneity might arise in part from consistently widespread yet variably patterned alterations in the connectivity of focal brain regions.

Methods—We used resting state functional connectivity magnetic resonance imaging to identify variable global dysconnectivity in 23 patients with DSM-IV SCZ relative to 22 age-, gender-, and parental socioeconomic status-matched control subjects with a novel global brain connectivity method that is robust to high variability across individuals. We examined cognitive functioning with a modified Sternberg task and subtests from the Wechsler Adult Intelligence Scale—Third Edition. We measured symptom severity with the Scale for Assessment of Positive and Negative Symptoms.

Results—We identified a dorsolateral prefrontal cortex (PFC) region with global and highly variable dysconnectivity involving within-PFC underconnectivity and non-PFC overconnectivity in patients. Variability in this “under/over” pattern of dysconnectivity strongly predicted the severity of cognitive deficits (matrix reasoning IQ, verbal IQ, and working memory performance) as well as individual differences in every cardinal symptom domain of SCZ (poverty, reality distortion, and disorganization).

Conclusions—These results suggest that global dysconnectivity underlies dorsolateral PFC involvement in the neuropathology of SCZ. Furthermore, these results demonstrate the possibility that specific patterns of dysconnectivity with a given network hub region might explain individual differences in symptom presentation in SCZ. Critically, such findings might extend to other neuropathologies with diverse presentation.

Keywords

fMRI; functional connectivity; global brain connectivity; prefrontal cortex; psychopathology; schizophrenia

A key challenge for understanding brain disorders is to identify sources of individual differences in symptom presentation. One plausible source of individual differences in

Address correspondence to Michael W. Cole, Ph.D., Psychology Department, Washington University, 1 Brookings Drive, Campus Box 1125, St. Louis, Missouri 63130; mwcole@mwcole.net..

The authors reported no biomedical financial interests or potential conflicts of interest.

Supplementary material cited in this article is available online.

symptoms is variability in brain dysconnectivity (1) (i.e., over-or underconnectivity relative to control subjects, as opposed to 'disconnectivity', which typically refers to underconnectivity alone) (2). Such dysconnectivity can be caused by a number of disease processes (3,4), and some of these processes likely alter connectivity differently across individuals, such that some brain regions might exhibit what we will refer to as variable global dysconnectivity (VGD). By this we mean highly variable (across individuals) dysconnectivity of a focal brain region with the rest of the brain. For example, if a disease process targets a given region as its connectivity is established during development, it could alter many connections of that region (reflected in relatively global dysconnectivity). However, the exact pattern of that dysconnectivity might vary across individuals, if the underlying disease process alters connectivity probabilistically and/or if the way in which the disease process alters connectivity interacts with other individual-specific variables. We hypothesized that variability in connectivity with regions exhibiting such VGD might be a source of individual differences in symptoms underlying some brain disorders. We used the substantial variability of symptom presentation in schizophrenia (SCZ) to test this hypothesis (5).

Schizophrenia symptoms vary along several domains—including reality testing; motor, emotional, and social abnormalities (6); as well as cognitive deficits (7). This disease has been repeatedly associated, neurobiologically, with disturbances in prefrontal cortex (PFC) (8). In addition to structural, neurochemical, and functional activation deficits in PFC (9,10), within-PFC dysconnectivity has been identified in intraregion circuits (11) and in larger across-region networks involving PFC (12,13). However, to our knowledge no systematic analysis of within-PFC global dysconnectivity—or its relation to individual differences in cognitive function and symptoms—has ever been conducted.

Here we searched for regions with global dysconnectivity with a recently developed global brain connectivity (GBC) method (14) restricted to PFC. This method uses resting state functional connectivity magnetic resonance imaging (fcMRI) (15) to search for globally connected or dysconnected brain regions in a data-driven manner and is able to reveal global disturbances in the connectivity of a brain region. Previous research has shown that resting state fcMRI estimates correlate highly with known functional brain networks (16) and structural connectivity (17). Unlike conventional seed or independent component analysis fcMRI methods—which can only identify patterns of (dys)connectivity that show the same spatial patterns across subjects—the GBC method is likely relatively unaffected by within-region and between-subject spatial variations in connectivity patterns (Figure S1 in Supplement 1). This makes GBC well-suited for testing hypotheses regarding VGD in heterogeneous brain disorders such as SCZ.

We hypothesized—on the basis of evidence of substantial disruption of PFC in SCZ—that individuals diagnosed with SCZ would exhibit VGD in a subset of regions within PFC. We identified focal regions expressing within-PFC global dysconnectivity and further tested the VGD hypothesis by quantifying variability in the connectivity of these focal regions throughout the brain. Finally, we hypothesized that, if VGD of these focal regions were relevant to psychopathology, then variability in their brain-wide fcMRI would strongly predict the severity of the cardinal symptoms of SCZ, including cognitive deficits as well as poverty, reality distortion, and disorganization symptoms.

Methods and Materials

Subject Recruitment

Subjects were recruited through the clinical core of the Conte Center for Neuroscience of Mental Disorders at Washington University in St. Louis. All subjects were interviewed by a

Master's level clinician and underwent the Structured Clinical Interview for DSMIV-TR and symptom ratings with the Scale for Assessment of Positive and Negative Symptoms (SAPS/SANS) (18,19). Control subjects were recruited with local advertisements in the same community as patients but were excluded if they had any lifetime history of Axis I psychiatric disorder or a first-degree relative with a psychotic disorder. Both control subjects and patients were excluded if they: 1) met criteria for DSM-IV substance abuse/dependence within the past 6 months or met criteria for present diagnosis of anxiety or depression; 2) had any severe medical conditions; 3) suffered head injury (past or present) with neurological symptoms or loss of consciousness; or 4) met DSM-IV diagnostic criteria of mental retardation. All SCZ subjects were medicated at the time of the scan and had to be receiving a stable level of medication for a period of at least 2 weeks (but most subjects were receiving the same dose of medication for 6 weeks or more). All but two patients were receiving atypical antipsychotic medication, and two patients receiving atypical medication also received typical antipsychotic medication.

Subjects provided informed consent approved by Washington University and were administered the Matrix Reasoning and Vocabulary sections of the Wechsler Adult Intelligence Scale—Third Edition (WAIS-III) (20). Working memory (WM) maintenance performance was assessed with a modified Sternberg task (21) involving abstract shapes at three levels of difficulty. Difficulty was varied on the basis of the similarity of target and distracter samples, and only the medium difficulty was used for subsequent correlation analyses, because it showed the largest between-group discrimination [80% correct for control subjects, 72% correct for patients; t (43) = 2.18, p = .03]. “Poverty” was quantified as the sum of flat affect, alogia, avolition, and anhedonia SANS subscores; “reality distortion” was the sum of hallucination and delusion SAPS subscores; and “disorganization” was the sum of bizarre behavior, positive formal thought disorder, and inattentiveness SAPS/SANS subscores.

Scanning

All subjects were scanned on a 3-T Tim TRIO scanner (Siemens Medical Solutions, Erlangen, Germany) at Mallinckrodt Institute of Radiology at the Washington University Medical School. Resting-state functional images were acquired with an asymmetrical spin-echo, echo-planar sequence, which was maximally sensitive to blood oxygenation level-dependent contrast (T2*) (repetition time = 2200 msec, echo time = 27 msec, field of view = 256 mm, flip = 90°, voxel size = 4 × 4 × 4 mm). Each run lasted for 7 min and contained 175 sets of oblique axial images (32 slices/volume), which were acquired parallel to the anterior–posterior commissure. Structural images were acquired with a sagittal magnetization prepared rapid gradient echo three-dimensional T1-weighted sequence (repetition time = 2400 msec, echo time = 3.16 msec, flip = 8°; voxel size = 1 × 1 × 1 mm).

Preprocessing

We preprocessed the functional magnetic resonance imaging (fMRI) data with the following steps: 1) slice-time correction, 2) removal of first five images from each run to reach steady state, 3) elimination of odd/even slice intensity differences due to interpolated acquisition, 4) rigid body motion correction, 5) intensity normalization to a whole brain mode value of 1,000 but without bias or gain field correction, 6) registration—with a 12-parameter affine transform—of the structural image to a template image in the Talairach coordinate system (22),and 7) coregistration of fMRI volumes to the structural image with resampling to 3 mm^3. Signal-to-noise ratio profiles (23,24) were calculated to ensure comparable signal-to-noise ratio across groups. See Methods in Supplement 1 for details.

Additionally, to remove possible sources of spurious correlations, all fMRI time-series were further preprocessed. These steps included: 1) high-pass filtering with cutoff frequency .009 Hz to remove scanner drift; 2) removal of a set of nuisance regressors including signals from the ventricles, deep white matter, whole brain average, motion correction parameters, and first derivatives of these regressors; 3) low-pass filtering with cutoff frequency .08 Hz to remove scanner high-frequency noise; and 4) smoothing with a 6-mm spherical dilation of gray matter voxels (to avoid averaging nonbrain voxel noise with the gray matter).

Restricted GBC

The weighted GBC approach (14) was applied with AFNI (25) to resting state fMRI data within the gray matter mask of PFC of each subject, as defined by Freesurfer (26). This restricted global brain connectivity (rGBC) approach involved: 1) using each PFC voxel as a seed, 2) computing the Fisher *z*-transformed correlation of each voxel seed with all other PFC voxels, and 3) averaging these correlations for each seed and using the resulting value for each seed voxel in a new statistical map. The resulting map summarizes the average connectivity of every PFC voxel to all other PFC voxels. We assessed rGBC dysconnectivity with two-tailed independent samples *t* tests between patients and control subjects. We corrected for multiple comparisons with family-wise error cluster threshold correction (27) via AFNI's AlphaSim. We used the PFC anatomical mask for the rGBC analysis ($p < .05$ with α at .05 and cluster size of 84 voxels) and the whole brain anatomical mask for subsequent region-of-interest (ROI) seed map analyses ($p < .05$ with α at .05 and cluster size of 131 voxels). Caret 5.5 software (Washington University School of Medicine, Department of Anatomy and Neurobiology, St. Louis, Missouri) was used for visualization, and all results were projected to the population average landmark and surface-based atlas (28).

Probabilistic Dysconnectivity Maps

To explore the extent of variable dysconnectivity across patients, the connectivity with the globally dysconnected regions of each patient was compared with the control group, and each voxel was assigned the percentage of patients showing dysconnectivity. See Methods in Supplement 1 for details.

Results

Participant Characteristics

The demographic data for the individuals with DSM-IVSCZ ($n = 23$) and healthy control subjects ($n = 22$) are presented in Table 1. Briefly, the groups were matched in terms of handedness, gender, age, parental education, and socioeconomic status. However, patients were impaired relative to control subjects on nonverbal (WAIS-III Matrix Reasoning) IQ, verbal (WAIS-III Vocabulary) IQ, and modified Sternberg WM performance. Patients also showed presence of symptoms across all cardinal domains (assessed with SAPS/SANS).

Within-PFC Global Dysconnectivity Associated with SCZ

We tested the hypothesis that SCZ involves within-PFC dysconnectivity by applying the weighted GBC approach (14) restricted to PFC. This method involves selecting each PFC voxel and computing its mean correlation with all other PFC voxels. The resulting statistical map summarizes the amount of functional connectivity of every PFC voxel to the rest of PFC for each subject. Next, we compared patient versus control rGBC with independent samples *t* tests, which revealed two focal regions of reduced within-PFC connectivity in patients: 1) right dorsolateral prefrontal cortex (DLPFC), and 2) left inferior frontal junction (IFJ) (Figure 1A, Table 2). We also examined the distributions of PFC connectivity for each

group (Figure 1B), which confirmed that the observed group rGBC differences were primarily due to decreases in positive connectivity for patients relative to control subjects.

Consistent DLPFC Whole-Brain Functional Dysconnectivity Pattern

We next examined consistent patterns of dysconnectivity between the DLPFC and IFJ regions and the rest of the brain, by comparing patient and control whole-brain connectivity seed maps with the two PFC seeds identified in the aforementioned analysis (Figure 2 for DLPFC; Figure S3 in Supplement 1 for IFJ). The DLPFC showed, in contrast to reduced within-PFC connectivity, increased connectivity with posterior cortex in patients, primarily with sensory, semantic, and motor regions (Table 3). Exceptions to this included reduced connectivity to posterior cerebellum and right midtemporal cortex. As before, we examined the distributions of correlations with DLPFC for identified ROIs (Figure 2B), which confirmed that the posterior ROIs generally showed more positive correlations with DLPFC for patients. In contrast, for prefrontal ROIs, patients generally showed less positive correlations with DLPFC. Given that we found IFJ connectivity did not significantly correlate with SCZ symptoms (see following text), we included details on IFJ whole-brain dysconnectivity in Table S1 in Supplement 1.

Assessing Global Dysconnectivity After Removing Focal Dysconnectivity

Rather than providing evidence for dysconnectivity that is both global and variable, the aforementioned results might indicate that the rGBC results are due to several clusters that are consistently dysconnected across individuals. We examined this possibility by rerunning the rGBC analysis after removing all significant group-level clusters from the analysis for DLPFC (all PFC clusters in Table 3 were removed) and IFJ (all PFC clusters in Table S1 in Supplement 1 were removed) separately. To be conservative, we used a small volume PFC-only cluster threshold (84 voxels) when identifying group level significant clusters to be removed before rerunning rGBC. If our VGD hypothesis holds, we should still observe a significant rGBC effect when rerunning the analysis on this reduced set of voxels. We tested for that possibility in two ways. First, we computed whether the regions identified in the previous rGBC analysis still show significant differences between the two groups. As expected, the DLPFC region remained significantly underconnected with the rest of PFC (t =–3.0, p = .005) even after removing clusters showing significant dysconnectivity with DLPFC (Figure S2A in Supplement 1). The IFJ showed a similar result (t =–3.3, p = .002). Second, we recomputed the voxel-wise PFC-only rGBC results. Results again revealed DLPFC and IFJ regions that were virtually identical to the ROIs identified by the original rGBC analysis. Results of both tests confirm that DLPFC (and IFJ) within-PFC global dysconnectivity is not solely due to a specific pattern of dysconnectivity that is consistent across patients, suggesting the presence of VGD.

Variable DLPFC Whole-Brain Functional Dysconnectivity Patterns

We next examined the variability in DLPFC dysconnectivity across patients. The percentage of patients showing dysconnectivity with DLPFC is depicted for each voxel in Figures S2B and S2C in Supplement 1. These maps were created by comparing the DLPFC connectivity of each patient with the DLPFC connectivity of the control group with one-sample z tests. The maps indicate that DLPFC dysconnectivity is global (much of cortex is dysconnected with DLPFC when both positive and negative maps are considered) and highly variable (most voxels are dysconnected in fewer than 30% of patients, yet 20 of 23 patients had some significant overconnectivity and every patients had some significant underconnectivity), as expected. Similar results were obtained for IFJ (Figure S5 in Supplement 1).

Correlations of PFC and Non-PFC DLPFC Connectivity with Cognitive Measures and Symptoms

We hypothesized that the high variability in DLPFC dysconnectivity observed in the previous analysis would be related to individual differences in psychopathology. Furthermore, the observation of differences between DLPFC (and IFJ) within-PFC and non-PFC dysconnectivity in the previous analyses led us to ask whether these distinct patterns of connectivity might differentially contribute to SCZ symptoms. To test these hypotheses, we computed: 1) average DLPFC and IFJ within-PFC connectivity, and 2) average DLPFC and IFJ non-PFC connectivity. We found that these connectivity values differed between patients and control subjects (Table S2 in Supplement 1), except for IFJ non-PFC connectivity. Next, we examined whether these PFC and non-PFC connectivity values correlated with individual differences in cognitive deficits and SAPS/SANS symptoms.

Only the cognitive measures correlated significantly and in patients only—with average DLPFC connectivity to PFC and non-PFC (Figure 3). The DLPFC within-PFC average connectivity was positively correlated with both matrix reasoning (r = .59, p = .003, CI = .23 to .80) and vocabulary (r = .45, p = .03, CI = .04 to .73) but not with WM performance (r = .14, p = .5). In contrast, DLPFC non-PFC average connectivity negatively correlated with matrix reasoning (r = –.52, p = .01, CI = –.76 to –.13), vocabulary (r = –.49, p = .02, CI = –.75 to –.10), and WM performance (r = –.50, p = .01, CI = –.76 to –.12). All significant regressions remained statistically significant when chlorpromazine-equivalent drug dosage, poverty, disorganization, and reality distortion measures were each separately included as covariates, and these measures did not make a significant contribution to any of these regressions (p > .27). These results suggest that cognitive deficits in patients might be associated with a pattern of both DLPFC-to-PFC underconnectivity and DLPFC-to-non-PFC overconnectivity.

Average correlations between IFJ and either PFC or non-PFC did not significantly correlate with any cognitive measures or SAPS/SANS symptoms.

DLPFC Brain-Wide Connectivity Correlations with Cognitive Measures and Symptoms

In contrast to the focus on average PFC versus non-PFC connectivity in the previous analysis, we also investigated the relationship between voxel-wise patterns of DLPFC/IFJ connectivity and cognitive measures as well as SAPS/SANS symptoms (Figure 4). Correlations were computed between each symptom domain measure and DLPFC/IFJ connectivity to each voxel. In other words, we computed a correlation between each symptom domain and each voxel's fcMRI connectivity with DLPFC (or IFJ) across patients. These analyses revealed robust patterns of connectivity that were reliably associated with symptom severity at the whole-brain level, across all three cognitive measures (Table S3 in Supplement 1) and all three symptom domains (Table S4 in Supplement 1). In contrast to DLPFC, IFJ connectivity only showed a correlation between disorganization and a single region in visual cortex (Table S5 in Supplement 1). Analyses of covariance including chlorpromazine-equivalent drug dosage, symptoms (for the cognitive correlations), and cognitive measures (for the symptom correlations) as covariates revealed that the results remained significant after these factors were accounted for. See Results in Supplement 1 for details.

Positive correlations between DLPFC connectivity and the poverty symptom domain were present in a motor network (M1/S1, presupplementary motor area, anterior cerebellum, and posterior putamen), whereas negative correlations were present in medial prefrontal cortex (MPFC) and precuneus/posterior cingulate cortex. The reality distortion symptom domain positively correlated with DLPFC connectivity to occipital regions and the frontal pole,

whereas it negatively correlated with supplementary motor area (SMA) and a cluster including S1, M1, and inferior parietal lobe. Finally, disorganization symptom severity positively correlated with DLPFC connectivity to left middle temporal lobe (Wernicke's area), S1/S2/M1, and frontal pole, whereas it was negatively correlated with right posterior DLPFC and premotor cortex. Taken together, these results show that variability in DLPFC fcMRI abnormalities was associated with symptom severity across all cardinal symptom domains.

Discussion

We hypothesized that VGD contributes to individual differences in SCZ symptoms. We identified two PFC regions—right DLPFC and left IFJ—with global dysconnectivity. Consistent with our predictions, variability in the dysconnectivity of one of these regions—DLPFC—was strongly correlated with cognitive deficits and every cardinal symptom domain. We also identified, in addition to VGD, a consistent pattern of aberrant DLPFC coupling in patients involving underconnectivity within PFC but overconnectivity with posterior sensory, motor, and semantic cortical regions. Furthermore, variability in this "under/over" pattern of DLPFC dysconnectivity across patients was associated with the severity of both cognitive impairments and cardinal symptoms, suggesting that further characterization of this DLPFC dysconnectivity pattern might be critical for understanding the pathophysiology of SCZ.

A variety of possible genetic and/or environmental disease processes are thought to underlie brain disorders such as SCZ (3), major depression (29), and autism (30). Finding evidence of VGD here suggests that some disease processes can variably affect the global dysconnectivity of a focal region. Examples of neuropathology that might variably affect the global dysconnectivity of a focal region include abnormalities in genetics specifying regional connectivity (31), insults during critical periods of the development of a brain region (32), and/or neurotransmitter system disruption (33,34).

Given that many SCZ abnormalities are not specific to DLPFC, it might be unclear why DLPFC shows greater global dysconnectivity and is more tightly associated with SCZ symptoms than other PFC regions. Multiple lines of evidence have implicated DLPFC as among the most highly globally connected "hub" brain regions (15,35). Given that such hubs exhibit extensive functional integration with the rest of the brain, they might be especially vulnerable to spreading and receiving disruptions to/from many potential sources (36). Supporting this conclusion, it has been suggested that DLPFC might use its extensive connectivity to implement a wide variety of complex cognitive control processes (14,37), many of which are compromised in SCZ (38).

Critically, we found that DLPFC was underconnected within PFC in patients. This is consistent with a variety of PFC abnormalities previously identified in SCZ. For instance, a recent meta-analysis of diffusion MRI studies identified consistent reductions of PFC white matter tracts in SCZ patients relative to control subjects (39), which are likely reflected in fcMRI estimates (17). Decreased dopaminergic tone in PFC could, from a neurotransmitter systems perspective, contribute to less within-PFC coordination (40) and greater noise in PFC due to increased random spiking of PFC neurons (34). Similarly, *N*-methyl-D-aspartic acid hypofunction in patients (33) might reduce coherent bursting (41) and sustained (42) activity in PFC, contributing to an overall reduction in coordinated neuronal communication. Such disruptions in PFC connectivity might in turn contribute to cognitive deficits via reduced integration with DLPFC. We demonstrate that, consistent with this possibility, the magnitude of DLPFC underconnectivity was strongly associated with impairments in both verbal and nonverbal IQ.

DLPFC overconnectivity with posterior regions was also associated with cognitive deficits. It was less clear how to interpret these findings on the basis of the existing literature, though previous studies have also identified a combination of decreased and increased connectivity in the brains of SCZ patients (12) (see Gaspar *et al.* [43] for review). The increased connectivity seen here might reflect aberrant influences of posterior regions on PFC, PFC on posterior regions, or both. First, increased posterior-to-PFC connectivity might reflect sensory inputs interfering with PFC function, exacerbating cognitive deficits. In contrast, increased PFC-to-posterior connectivity might reflect DLPFC-mediated attempts to reduce noise stemming from neurotransmitter abnormalities in posterior regions (44) via (possibly faulty) top-down control (45). However, these top-down signals might actually amplify noise by aberrantly biasing posterior cortical areas, possibly exacerbating cognitive deficits and symptoms. One speculative possibility is that this might result in a vicious cycle in which increasing attempts to compensate lead to increased noise that exacerbates symptom expression. Further research is necessary to assess these possibilities.

Importantly, we also found that DLPFC dysconnectivity correlated with every cardinal symptom domain of SCZ. Prospective testing is needed to further elucidate the complex constellations of connectivity correlating with specific symptoms. However, present results suggest that DLPFC dysconnectivity might play a central role in the disease processes underlying cardinal SCZ symptoms. Furthermore, the patterns of symptom correlations are generally consistent with the within-PFC underconnectivity and non-PFC overconnectivity pattern observed in the cognitive findings discussed in the preceding text. Overall, these results suggest that characterizing the mechanisms behind the observed under/over dysconnectivity pattern might provide key insights into the neurophysiology of SCZ.

The anatomical differentiation of the connections correlating with different symptoms suggests the general under/over dysconnectivity pattern might have different functional consequences, depending on the specific circuits involved. For instance, decreased DLPFC connectivity with SMA was associated with increased reality distortion symptoms, possibly due to reduced self-monitoring by SMA creating the illusion that self-generated thoughts and percepts have external sources (46) (i.e., hallucinations). Furthermore, correlations between reality distortion and increased DLPFC with posterior sensory region connectivity are consistent with suggestions that some reality distortions originate from overly strong—and dysfunctional—top-down signals upon sensory regions (47,48), possibly originating in right DLPFC (49).

Greater disorganization severity was associated with stronger DLPFC to Wernicke's area connectivity and decreased DLPFC connectivity with other lateral PFC regions, in contrast to the circuits correlating with reality distortion. This might reflect, in line with the observed under/over dysconnectivity pattern, aberrant linguistic/cognitive processing due to: 1) decreased DLPFC connectivity with lateral PFC regions thought to be important for language/cognition (50); and 2) as argued in the preceding text, an attempt to compensate for increased noise in Wernicke's area by increased—but dysfunctional—top-down control.

Lastly, we also found that greater poverty symptom severity was associated with weaker DLPFC connectivity with MPFC and posterior cingulate and stronger DLPFC connectivity with motor/somatosensory cortex. Again in line with the observed under/over dysconnectivity pattern, this might reflect: 1) decreased DLPFC involvement with emotion processes in MPFC leading to altered affect; and 2) noise in motor regions (due to widespread neurotrans mitter system defects) leading to compensatory overcontrol by DLPFC and consequent alterations in aspects of motor function included in the poverty domain (51).

Critically, present results demonstrate the utility of GBC for identifying both variable and consistent global dysconnectivity. Other recently developed graph theoretical approaches (52–54) have typically either: 1) required extensive within-group similarity in the exact patterns of connectivity to identify differences between patients and control subjects (ruling out connections with substantial individual differences) (see Figure S1 in Supplement 1), or 2) involved summary statistics (e.g., path length) that reflect general systemic dysfunction rather than network-specific or region-specific dysfunction (which might lend clues regarding the origins of systemic dysfunction). A recent graph theoretical study identified some region-specific alterations in GBC (55), yet they did not take the further step of characterizing the underlying connectivity patterns contributing to that result (essential to the present findings; e.g., identifying the within-PFC underconnectivity pattern that led to the GBC result in DLPFC).

In conclusion, disease processes that lead to VGD of focal brain regions—especially regions that are functionally integrated network hubs—might be present in a variety of neuropsychiatric diseases. We found a substantial amount of symptom-related variability in DLPFC dysconnectivity patterns across SCZ patients, supporting this possibility. Thus, extending GBC to other neuropsychiatric conditions might confer great utility for identifying areas exhibiting global dysconnectivity relevant to individual differences in psychopathology.

Supplementary Material

Refer to Web version on PubMed Central for supplementary material.

Acknowledgments

This study was supported by the McDonnell Center for Systems Neuroscience. We would like to thank staff at the Conte Center for Neuroscience of Mental Disorders for their help in recruiting participants and collecting data as well as Todd Braver and Phil Corlett for insightful comments and suggestions.

References

1. He BJ, Snyder AZ, Vincent JL, Epstein A, Shulman GL, Corbetta M. Breakdown of functional connectivity in frontoparietal networks underlies behavioral deficits in spatial neglect. Neuron. 2007; 53:905–918. [PubMed: 17359924]
2. Stephan KE, Baldeweg T, Friston KJ. Synaptic plasticity and dysconnection in schizophrenia. Biol Psychitary. 2006; 59:929–939.
3. Karlsgodt KH, Sun D, Jimenez AM, Lutkenhoff ES, Willhite R, van Erp TGM, Cannon TD. Developmental disruptions in neural connectivity in the pathophysiology of schizophrenia. Dev Psychopathol. 2008; 20:1297–1327. [PubMed: 18838043]
4. Kumar A, Cook IA. White matter injury, neural connectivity and the pathophysiology of psychiatric disorders. Dev Neurosci. 2002; 24:255–261. [PubMed: 12457063]
5. Macdonald AW, Schulz SC. What we know: Findings that every theory of schizophrenia should explain. Schizophr Bull. 2009; 35:493–508. [PubMed: 19329559]
6. Kay S, Flszbein A, Opfer L. The Positive and Negative Syndrome Scale (PANSS) for schizophrenia. Schizophr Bull. 1987; 13:261–276. [PubMed: 3616518]
7. Elvevag B, Goldberg T. Cognitive impairment in schizophrenia is the core of the disorder. Crit Rev Neurobiol. 2000; 14:1–22. [PubMed: 11253953]
8. Goldman-Rakic PS. Working memory dysfunction in schizophrenia. J Neuropsychiatr. 1994; 6:348–357.
9. Eisenberg DP, Berman KF. Executive function, neural circuitry, and genetic mechanisms in schizophrenia. Neuropsychopharmacology. 2010; 35:258–277. [PubMed: 19693005]

10. MacDonald AW, Carter CS, Kerns JG, Ursu S, Barch DM, Holmes AJ, et al. Specificity of prefrontal dysfunction and context processing deficits to schizophrenia in never-medicated patients with first-episode psychosis. Am J Psychiatry. 2005; 162:475–484. [PubMed: 15741464]
11. Lewis DA, Hashimoto T, Volk DW. Cortical inhibitory neurons and schizophrenia. Nat Rev Neurosci. 2005; 6:312–324. [PubMed: 15803162]
12. Zhou Y, Liang M, Jiang T, Tian L, Liu Y, Liu Z, et al. Functional dysconnectivity of the dorsolateral prefrontal cortex in first-episode schizophrenia using resting-state fMRI. Neurosci Lett. 2007; 417:297–302. [PubMed: 17399900]
13. Rotarska-Jagiela A, van de Ven V, Oertel-Knöchel V, Uhlhaas PJ, Vogeley K, Linden DE. Resting-state functional network correlates of psychotic symptoms in schizophrenia. Schizophr Res. 2010; 117:21–30. [PubMed: 20097544]
14. Cole MW, Pathak S, Schneider W. Identifying the brain's most globally connected regions. Neuroimage. 2010; 49:3132–3148. [PubMed: 19909818]
15. Fox MD, Greicius M. Clinical applications of resting state functional connectivity. Front Syst Neurosci. 2010; 4:19. [PubMed: 20592951]
16. Cordes D, Haughton V, Arfanakis K, Wendt G, Turski P, Moritz C, et al. Mapping functionally related regions of brain with functional connectivity MR imaging. AJNR Am J Neuroradiol. 2000; 21:1636–1644. [PubMed: 11039342]
17. Honey CJ, Sporns O, Cammoun L, Gigandet X, Thiran JP, Meuli R, Hagmann P. Predicting human resting-state functional connectivity from structural connectivity. Proc Natl Acad Sci U S A. 2009; 106:2035–2040. [PubMed: 19188601]
18. Andreasen, NC. The Scale for the Assessment of Negative Symptoms (SANS). University of Iowa; Iowa City: 1983.
19. Andreasen, NC. The Scale for the Assessment of Positive Symptoms (SAPS). University of Iowa; Iowa City: 1983.
20. Wechsler, D. Wechsler Adult Intelligence Scale—Third Edition. Psychological Corporation; San Antonio: 1997.
21. Sternberg S. The discovery of processing stages: Extensions of Donders' method. Acta Psychol. 1969; 30:276–315.
22. Talairach, J.; Tournoux, P. Co-Planar Stereotaxic Atlas of the Human Brain. Thieme; New York: 1988.
23. LaBar K, Gitelman D, Mesulam M, Parrish T. Impact of signal-to-noise on functional MRI of the human amygdala. Neuroreport. 2001; 12:3461. [PubMed: 11733691]
24. Parrish TB, Gitelman DR, LaBar KS, Mesulam MM. Impact of signal-to-noise on functional MRI. Magn Reson Med. 2000; 44:925–932. [PubMed: 11108630]
25. Cox RW. AFNI: Software for analysis and visualization of functional magnetic resonance neuroimages. Comput Biomed Res. 1996; 29:162–173. [PubMed: 8812068]
26. Desikan RS, Ségonne F, Fischl B, Quinn BT, Dickerson BC, Blacker D, et al. An automated labeling system for subdividing the human cerebral cortex on MRI scans into gyral based regions of interest. Neuroimage. 2006; 31:968–980. [PubMed: 16530430]
27. Forman SD, Cohen JD, Fitzgerald M, Eddy WF, Mintun MA, Noll DC. Improved assessment of significant activation in functional magnetic resonance imaging (fMRI): Use of a cluster-size threshold. Magn Reson Med. 1995; 33:636–647. [PubMed: 7596267]
28. Van Essen DC. A Population-Average, Landmark- and Surface-based (PALS) atlas of human cerebral cortex. Neuroimage. 2005; 28:635–662. [PubMed: 16172003]
29. Roy MA, Neale MC, Pedersen NL, Mathé AA, Kendler KS. A twin study of generalized anxiety disorder and major depression. Psychol Med. 1995; 25:1037–1049. [PubMed: 8588001]
30. Geschwind D, Levitt P. Autism spectrum disorders: Developmental disconnection syndromes. Curr Opin Neurobiol. 2007; 17:103–111. [PubMed: 17275283]
31. Meyer-Lindenberg A. Neural connectivity as an intermediate phenotype: Brain networks under genetic control. Hum Brain Mapp. 2009; 30:1938–1946. [PubMed: 19294651]
32. Brown AS, Derkits EJ. Prenatal infection and schizophrenia: A review of epidemiologic and translational studies. Am J Psychiatry. 2010; 167:261–280. [PubMed: 20123911]

33. Olney JW, Newcomer JW, Farber NB. NMDA receptor hypofunction model of schizophrenia. J Psychiatr Res. 1999; 33:523–533. [PubMed: 10628529]
34. Winterer G, Weinberger DR. Genes, dopamine and cortical signal-to-noise ratio in schizophrenia. Trends Neurosci. 2004; 27:683–690. [PubMed: 15474169]
35. Modha DS, Singh R. Network architecture of the long-distance pathways in the macaque brain. Proc Natl Acad Sci U S A. 2010; 107:13485–13490. [PubMed: 20628011]
36. Bullmore E, Sporns O. Complex brain networks: Graph theoretical analysis of structural and functional systems. Nat Rev Neurosci. 2009; 10:186–198. [PubMed: 19190637]
37. Cole MW, Schneider W. The cognitive control network: Integrated cortical regions with dissociable functions. Neuroimage. 2007; 37:343–360. [PubMed: 17553704]
38. Barch DM. The cognitive neuroscience of schizophrenia. Annu Review Clin Psychol. 2005; 1:321–353.
39. Ellison-Wright I, Bullmore E. Meta-analysis of diffusion tensor imaging studies in schizophrenia. Schizophr Res. 2009; 108:3–10. [PubMed: 19128945]
40. Braver TS, Barch DM, Cohen JD. Cognition and control in schizophrenia: A computational model of dopamine and prefrontal function. Biol Psychiatry. 1999; 46:312–328. [PubMed: 10435197]
41. Jackson ME, Homayoun H, Moghaddam B. NMDA receptor hypofunction produces concomitant firing rate potentiation and burst activity reduction in the prefrontal cortex. Proc Natl Acad Sci USA. 2004; 101:8467–8472. [PubMed: 15159546]
42. Wang XJ. Synaptic reverberation underlying mnemonic persistent activity. Trends Neurosci. 2001; 24:455–463. [PubMed: 11476885]
43. Gaspar, P.; Bosman, C.; Ruiz, S.; Aboitiz, F. Aboitiz, F., editor. The aberrant connectivity hypothesis in schizophrenia.; Attention to Goal-Directed Behavior. 2008. p. 301-323.
44. Rolls ET, Loh M, Deco G, Winterer G. Computational models of schizophrenia and dopamine modulation in the prefrontal cortex. Nat Rev Neurosci. 2008; 9:696–709. [PubMed: 18714326]
45. Fuster J. The prefrontal cortex—an update: Time is of the essence. Neuron. 2001; 30:319–333. [PubMed: 11394996]
46. Frith C. The neural basis of hallucinations and delusions. C R Biol. 2005; 328:169–175. [PubMed: 15771003]
47. Corlett PR, Frith CD, Fletcher PC. From drugs to deprivation: A Bayesian framework for understanding models of psychosis. Psychopharmacology (Berl). 2009; 206:515–530. [PubMed: 19475401]
48. Fletcher PC, Frith CD. Perceiving is believing: A Bayesian approach to explaining the positive symptoms of schizophrenia. Nat Rev Neurosci. 2009; 10:48–58. [PubMed: 19050712]
49. Corlett PR, Murray GK, Honey GD, Aitken MRF, Shanks DR, Robbins TW, et al. Disrupted prediction-error signal in psychosis: Evidence for an associative account of delusions. Brain. 2007; 130:2387–2400. [PubMed: 17690132]
50. Weiss EM, Hofer A, Golaszewski S, Siedentopf C, Felber S, Fleischhacker WW. Language lateralization in unmedicated patients during an acute episode of schizophrenia: A functional MRI study. Psychiatry Res. 2006; 146:185–190. [PubMed: 16530393]
51. Fenton W, Wyatt R, McGlashan T. Risk factors for spontaneous dyskinesia in schizophrenia. Arch Gen Psychiatry. 1994; 51:643. [PubMed: 8042913]
52. Bassett DS, Bullmore E, Verchinski BA, Mattay VS, Weinberger DR, Meyer-Lindenberg A. Hierarchical organization of human cortical networks in health and schizophrenia. J Neurosci. 2008; 28:9239–9248. [PubMed: 18784304]
53. Liu Y, Liang M, Zhou Y, He Y, Hao Y, Song M, et al. Disrupted small-world networks in schizophrenia. Brain. 2008; 131:945–961. [PubMed: 18299296]
54. Micheloyannis S, Pachou E, Stam C, Breakspear M, Bitsios P, Vourkas M, et al. Small-world networks and disturbed functional connectivity in schizophrenia. Schizophr Res. 2006; 87:60–66. [PubMed: 16875801]
55. Lynall M-E, Bassett DS, Kerwin R, McKenna PJ, Kitzbichler M, Muller U, Bullmore E. Functional connectivity and brain networks in schizophrenia. J Neurosci. 2010; 30:9477–9487. [PubMed: 20631176]

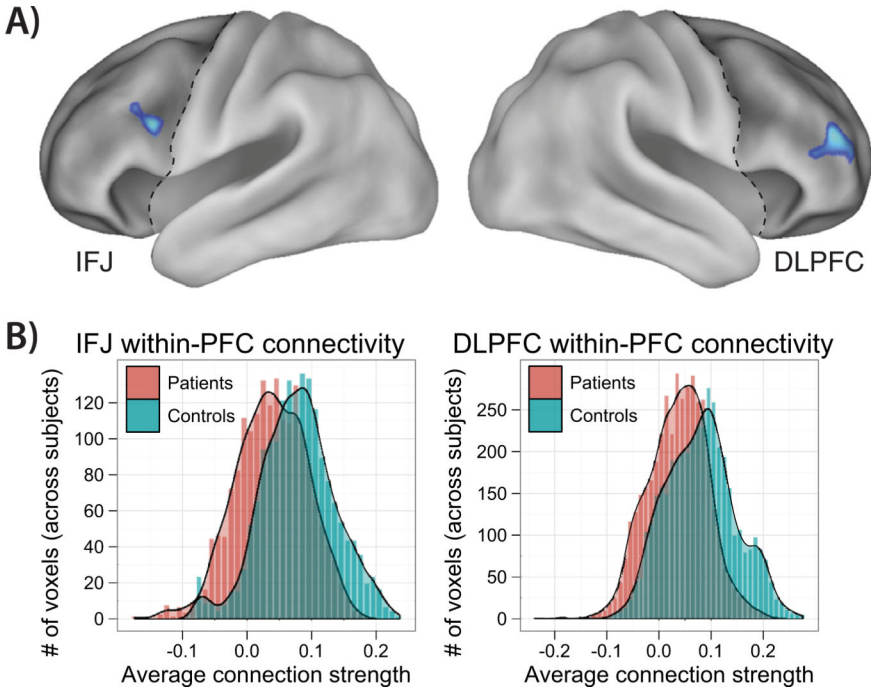

Figure 1.

Within–prefrontal cortex (PFC) dysconnectivity in schizophrenia. **(A)** The weighted global brain connectivity method (14) was used to assess within-PFC dysconnectivity, which involves assigning each voxel its average connectivity to all other voxels. Two regions—right dorsolateral prefrontal cortex (DLPFC) and left inferior frontal junction (IFJ)—showed reduced within-PFC connectivity for patients compared with control subjects. **(B)** The average connection strengths for each voxel within the two regions are depicted in histograms. The between-group shift in distributions indicates both decreased positive connectivity and increased negative connectivity for patients. See Figure S4 in Supplement 1 for the basic connectivity pattern of the DLPFC region.

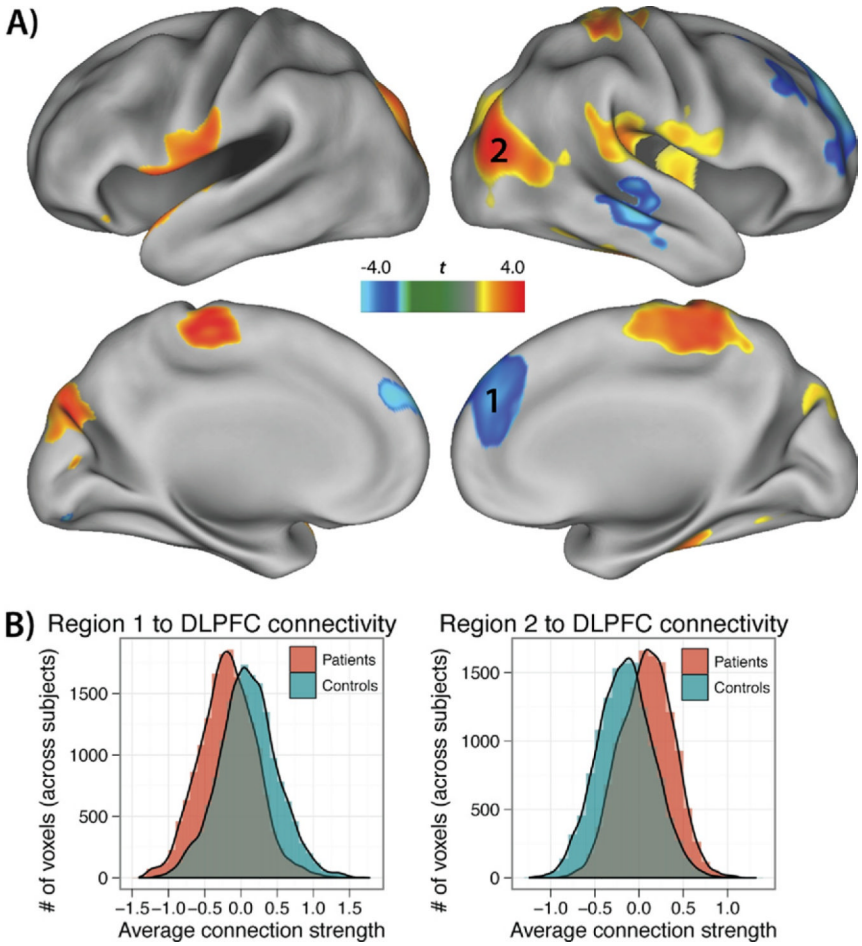

Figure 2.

The DLPFC is underconnected with prefrontal cortex and overconnected with posterior cortex in schizophrenia (SCZ). **(A)** Individuals with SCZ had significantly reduced DLPFC connectivity with several other PFC regions compared with control subjects. In contrast, individuals with SCZ had significantly increased DLPFC connectivity with several regions of posterior cortex (except for right midtemporal cortex and posterior cerebellum), predominantly involving primary and secondary sensory regions. **(B)** Two representative regions are shown to illustrate the positive/negative shift in DLPFC connectivity for patients relative to control subjects. Region 1 is medial, superior, and anterior PFC, whereas Region 2 is superior occipital gyrus. See Figure S3 in Supplement 1 for the equivalent figure with inferior frontal junction as the seed region. Abbreviations as in Figure 1.

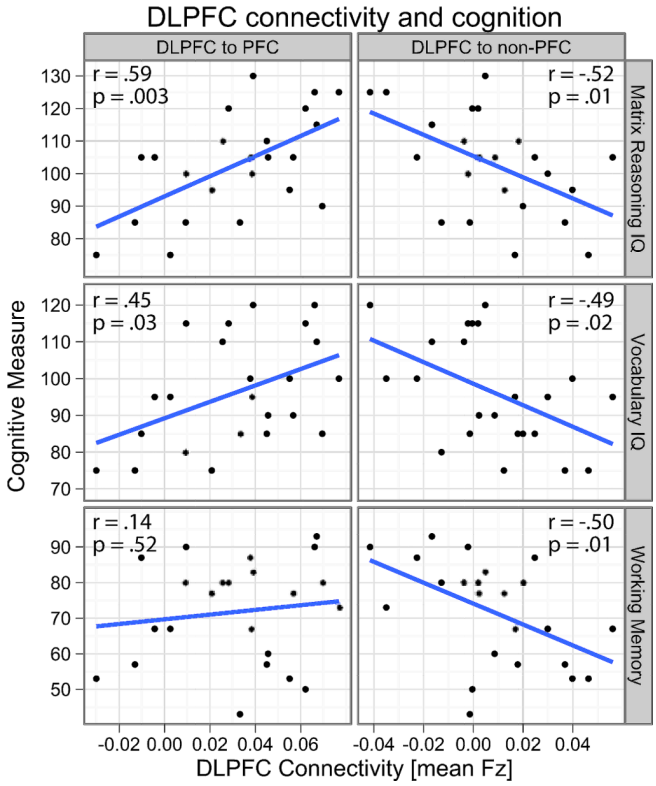

Figure 3.

The DLPFC connectivity correlates with cognitive measures differentially for PFC and posterior cortex. Three cognitive measures (Wechsler Adult Intelligence Scale [WAIS] matrix IQ, WAIS vocabulary IQ, and working memory [WM] task accuracy) and three symptom domain measures (poverty, reality distortion, and disorganization) were included in a DLPFC-connectivity correlation analysis. Only the cognitive measures correlated significantly with the within-PFC/non-PFC DLPFC connectivity estimates ($p < .05$, false discovery rate corrected for multiple comparisons). None of these correlations were statistically significant in control subjects. This pattern of correlations is consistent with the pattern of DLPFC dysconnectivity (Figure 2) in that the more the connectivity patterns of patients resemble that of the control subjects, the more their cognitive abilities look like those of the control subjects. In other words, improved cognition is predicted by increased connectivity with underconnected PFC as well as decreased connectivity with overconnected posterior cortex. Abbreviations as in Figure 1.

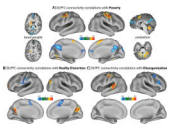

Figure 4.
Dorsolateral prefrontal cortex (DLPFC) connectivity correlates with all symptom domains of schizophrenia. The DLPFC connectivity correlations with symptoms and cognitive measures were assessed across all voxels. All symptom domains (and cognitive measures) (Table S3 in Supplement 1) were significantly correlated with multiple regions ($p < .05$, family-wise error corrected). In contrast, inferior frontal junction connectivity only correlated with disorganization in a single region (Table S5 in Supplement 1). These results demonstrate the utility of global brain connectivity for localizing globally dysconnected regions with high individual variability related to individual differences in symptoms.

Table 1

Participant Characteristics

	Control Subjects		Patients		Significance[a]	
	M	**SD**	**M**	**SD**	***t*-Stat/χ^2**	***p***
Age (yrs)	37.18	7.59	36.54	9.36	.26	.800
Gender (% male)	74		79		.42	.679
Paternal Education (yrs)	12.70	1.46	13.58	3.01	1.28	.208
Maternal Education	12.48	1.53	13.61	3.04	1.59	.119
Paternal SES	21.59	8.92	27.39	11.17	1.91	.062
Maternal SES	17.27	8.55	25.68	11.78	2.69	.010
Education (yrs)	15.26	2.12	13.08	2.10	3.51	.001
Handedness (% right)	100.00		87.50		1.43	.158
WAIS Vocabulary IQ	110.23	10.85	96.30	14.79	3.55	.001
WAIS Matrix IQ	115.45	11.64	102.83	15.65	3.04	.004
Medication (CPZ equivalents)			589.88	550.59		
Mean SAPS Global Item Score	.02	.11	1.94	1.19	7.7	1e-7
Mean SANS Global Item Score	.37	.62	2.47	.79	9.9	1e-12
Disorganization	.78	1.17	5.33	2.75	7.2	5e-8
Poverty	1.13	2.39	10.33	3.48	10.4	1e-12
Reality Distortion	.00	.00	4.42	3.54	6.0	5e-6

SES, socioeconomic status; WAIS, Wechsler Adult Intelligence Scale; CPZ, chlorpromazine-equivalent drug dosage; SAPS, Scale for Assessment of Positive Symptoms; SANS, Scale for Assessment of Negative Symptoms.

[a]Significance of between group statistical tests.

Table 2

Within-PFC rGBC, Patients Versus Control Subjects

Region	*t*-Stat	Volume (3 mm^3)	Tal X	Tal Y	Tal Z	Area (s)
Right DLPFC	–2.42	193	48.6	41.7	17.2	46, 45, 10
Left IFJ	–2.40	84	–41.9	6.8	24.4	9, 6

PFC, prefrontal cortex; rGBC, restricted global brain connectivity; Tal, Talairach coordinate system; DLPFC, dorsolateral prefrontal cortex; IFJ, inferior frontal junction.

Table 3

Whole-Brain DLPFC Connectivity Differences Between Patients and Control Subjects

Region	*t*-Stat	Volume (3 mm^3)	Tal X	Tal Y	Tal Z	Area(s)
Underconnected						
Medial/superior/anterior PFC	–2.66	732	13.4	45.5	29.2	8, 9, 10
Left posterior cerebellum	–2.44	231	–23.1	–79.7	–31.7	—
Right posterior DLPFC, superior frontal	–2.43	224	36.1	18.7	56.4	8, 9, 6
Right mid temporal gyrus	–2.69	164	59	–27	–8.6	21, 20
Left PMC[a]	–2.49	116	–37.5	4.0	46.6	6
Right ventrolateral PFC[a]	–2.46	107	40.2	23.8	–7.0	47, 13
Subcallosal cingulate[a]	–2.50	92	–8.1	19.3	–16.1	11, 25
Overconnected						
Right superior occipital gyrus	2.65	585	41.1	–78.5	18	19
Medial S1/S2	2.66	478	9	–34.7	58.9	5, 3, 2
Left cuneus	2.46	249	–18.1	–86.1	25.2	18, 19
Right insula/A1/A2/PMC	2.42	246	43.2	–13.9	17.4	13, 41, 6
Left temporal lobe/S1/M1	2.55	244	–54.9	–1.6	4.3	22, 43, 38, 3, 1, 4
Right A1/A2	2.46	186	64.5	–31.4	17.2	41, 42, 22
Right parahippocampus/fusiform	2.55	141	38.5	–41.9	–12.8	36, 20

PMC, premotor cortex; other abbreviations as in Table 2.

[a]With within-PFC family-wise error correction for multiple comparisons.